



# Experimental and Numerical Investigations of Using Nanoparticles in Groundwater Remediation

Ahmed S. Okasha<sup>1</sup> · Mohamed A. Abd-Elmegeed<sup>1</sup> · Ahmed E. Hassan<sup>1</sup>

Received: 11 March 2022 / Accepted: 31 July 2022 / Published online: 18 August 2022  
© The Author(s) 2022

## Abstract

The efficiency of using zeolite nano-clay and silica sand in removing iron from groundwater is investigated experimentally as an application of in situ remediation technique using permeable reactive barrier (PRB). In the first stage of the study batch experiments were conducted on coarse silica sand and fine silica gravel to determine their iron removal efficiency from contaminated water. The results showed that the removal efficiency was about 51.90% for coarse silica sand while fine silica gravel failed to reduce the iron concentration in water. A mix of zeolite nano-clay and coarse silica sand with a ratio of 1:30 was tested. It was found that iron removal efficiency significantly increases to about 99.70%. The linear adsorption isotherm was found to be the most representative for the adsorption of iron onto coarse silica sand and the mix of nano-clay and coarse silica sand with distribution coefficients equal 0.0009 and 0.001, respectively. In the second stage a glass sand tank with coarse silica sand and a mix of zeolite nano-clay and coarse silica PRBs was constructed. The sand tank was used to investigate the effect of sampling time, head difference, iron concentration, nano-clay dosage, and thickness of permeable reactive barrier on the iron removal efficiency. The results indicated that increasing iron concentration and head difference decreases iron removal efficiency. The mix of zeolite nano-clay and coarse silica sand improves iron removal efficiency. Furthermore, increasing nano-clay dosage slightly increases the removal efficiency. However, increasing the thickness of filter layer (i.e., PRB) significantly improves the removal efficiency. Finally, the experimental model data were used to test the capability of a numerical contaminant transport model to predict the removal efficiency. The MT3DMS numerical model included within the Groundwater Modeling System (GMS) was used along with the different experimental data to obtain reaction rate values as calibration parameters for linear isotherm. Reaction rates that yield modeling results matching experimental data were obtained.

**Keywords** Nanotechnology · Preamble reactive barrier · Groundwater remediation · Nano-clay

## 1 Introduction

Iron exists with significant amounts in earth's crust. It also exists naturally in water with low concentrations in two forms: the complex form like ferric iron and the soluble form like ferrous iron. It could also have an industrial origin (e.g.,

iron and steel industry, metals corrosion and mining activities). High iron concentrations change the water appearance and color to red in addition to giving the water a metallic taste and unpleasant odor. Not to mention the toxicity if it exists with very high concentrations to humans, animals, aquatic life, and plants. It also causes corrosion to drains' sewers because of the development of ferro-bacteria and microorganisms leading to the reduction in pipe flow cross section, failure of water systems, and deteriorated water quality [1].

In the last two decades, groundwater remediation had been an active area of research. Many remediation techniques have been investigated which can be classified into two main categories: in situ and ex situ. One of the most effective and common in situ techniques is the permeable reactive barrier (PRB) [2]. It had been widely used in Europe

✉ Mohamed A. Abd-Elmegeed  
Mohamed.attia@cu.edu.eg

Ahmed S. Okasha  
ahmedshawkyokasha@eng.cu.edu.eg

Ahmed E. Hassan  
ahassan@eng.cu.edu.eg

<sup>1</sup> Irrigation and Hydraulics Department, Faculty of Engineering, Cairo University, Giza, Egypt



and America in the past 30 years. It includes the installation of PRB perpendicular to the direction of groundwater flow downstream the contamination. Then, pollutants that migrates with groundwater flow reacts with the active material chemically, physically, and biologically by adsorption, precipitation, redox reaction, and biodegradation to remove them from groundwater. The traditional methods, such as pump and treat method, have many disadvantages including the high cost, disturbance to the groundwater system and flow pattern, further diffusion of pollutants and short-term effect. The PRB method, on the other hand, has a number of advantages such as the low cost, small disturbance to groundwater, no need for external power, small secondary pollution, and long-term effect and operation [3].

Although natural silica can be used as the active material for the PRB for the removal of iron and zinc, it will not achieve high removal efficiency [4]. Nanotechnology has been a growing field of research in groundwater remediation. Due to their tiny size and large surface area, nanoparticles have special adsorption properties which enable them to be a proper material for the removal of heavy metals and organic pollutants from contaminated water and wastewater [5–7]. The size of Nanoparticles ranges from 1 to 100 nm. They are classified into two categories: man-made and natural nanoparticles. Man-made can be designed in labs and produced as by-products. On the other hand, natural nanoparticles can be of geogenic (resulting from geological processes), biogenic (produced by living organisms), pyrogenic (produced by heat or fever) or atmospheric origin. It is also classified by composition to carbon-based and inorganic [8, 9].

Many researchers investigated the efficiency of using several types of nanoparticles in groundwater remediation. Zhang [10] reviewed the use of nanoscale iron particles in groundwater remediation. He assessed developments in laboratory and pilot studies, such as reactivity of the nanoparticles towards contaminants in soil and water over extended periods of time, synthesis of nanoscale iron particles from Fe(II) and Fe(III), in situ reactions of the nanoparticles in the subsurface and field tests validating the injection of nanoparticles into aquifer. Lien and Zhang [11, 12] investigated in batch experiments the potential of using nanoscale bimetallic (Pd/Fe) particles in reducing chlorinated ethenes. They concluded that, the nanoscale bimetallic particles might be a treatment alternative for groundwater in situ remediation of chlorinated ethanes. Prabhakar and Bibi [13] presented a review for using nanotechnology for creating new and improved remediation techniques to clean up the environment. They clarified that nano-titanium dioxide is very effective catalyst and can be used for the treatment of water from organic pollutants. Nano-silver is used to disinfect drinking water. Nanoscale zero-valent iron is used in ex situ slurry reactors

for the treatment of contaminated soils, sediments, and solid wastes.

Carbon-based nanoparticles (CNM) are considered the most common nano-particles used in water remediation [14]. Single-walled carbon nanotubes (SWCNTs) were used on the removal of dissolved phenol compounds in industrial wastewater [15]. Multiwalled carbon nanotubes (MWCNTs) are used in the removal of trichloroethylene manganese and iron from groundwater using filtration [16, 17] or the removal of chromium (VI) from groundwater [18]. In recent years, nano-clay particles were used in water remediation such as Montmorillonite nano-clay (Mt) which was used in the removal of Cerium Ce (III) metal ion and Crystal Violet (CV) organic dye from wastewater through batch adsorption experiments [19]. Zeolite cotton is used in the removal of heavy metals from water through household water treatment filter [20]. All these materials can be adjusted by many processes such as oxidation and acidification to modify their properties. A variety of nanomaterials are being developed by researchers to use for in situ and ex situ groundwater remediation.

The main objective of this study is to investigate the efficiency of using zeolite nano-clay and silica sand in the removal of iron from groundwater using experimental setups. The setup is aimed at mimicking the application of in situ remediation via permeable reactive barrier (PRB). The experiments target identifying the factors that affect the removal efficiency to provide guidance on the best arrangement for field setup of PRB relying on such nanoparticles. Another goal of this study is to test the capability of a numerical contaminant transport model to predict the experimental results and obtain sorption isotherm coefficients.

## 2 Methodology

The objectives of this study were achieved through several steps. In the first step, batch experiments were conducted to determine the right size of silica sand to mix with nano-clay and their iron removal efficiency. An experimental three-dimensional sand box model simulating permeable reactive barrier (PRB) was built to identify the parameters that affect the removal efficiency and evaluate such effect. Finally, a numerical contaminant transport model simulating nanoparticles' effect on contaminated groundwater was developed to assess its capability to reproduce the experimental results and to obtain sorption isotherm coefficients.

### 3 Experimental Model Setup

#### 3.1 Materials

Silica sand has been widely used as the main media in filters for treating water used in swimming pools and household water consumed by humans. Due to its purity, metal free and high quality it achieves quite good removal efficiencies for heavy metals and organic pollutants [4]. In this study coarse silica sand (0.7–1.25 mm) and fine silica gravel (3–6 mm) are used to determine their iron removal efficiency from contaminated water. There are many types of clay minerals (e.g., zeolite, perlite, and montmorillonite) that are used for groundwater remediation. Zeolite has been previously used as the active material in PRB for the removal of heavy metals from groundwater. In this research, the efficiency of using a mix of zeolite nano-clay and silica sand in removing iron from groundwater is investigated. Iron sulfate salt was used to produce iron solutions with different concentrations which acts as iron contaminated groundwater in present study.

#### 3.2 Batch Experiments

Batch experiments were conducted on two types of silica, coarse silica sand (0.7–1.25 mm) and fine silica gravel (3–6 mm) to investigate their iron removal efficiency. A volume of 0.55 L of iron solutions with concentrations ranging from 15 to 70 mg/l were added to 552.16 gm of coarse silica sand and fine silica gravel. Vibratory sieve shaker was used to shake the batch samples. The device was set on 50 amplitudes for all samples. Samples were shaken for 60 min and were left for 24 h to settle down. Final solutions of volume 0.1 L were extracted from all the samples.

A mass of 18.41 gm of zeolite nano-clay were mixed with 533.76 gm of coarse silica sand (1:30). A volume of 0.55 L of iron solutions with concentrations ranging from 30 to 70 mg/l were added to the mix. The same procedure presented above is followed till extracting the final solutions from all samples. A 22 batch experiments were conducted on all types of soils. Figure 1 shows batch experiments on coarse silica sand and mix of zeolite nano-clay with coarse silica sand 1:30 with different concentrations of iron solutions.

#### 3.3 Sand Tank Experiments

A tempered glass tank 6 mm thickness was built with dimensions of 140 cm length, 75 cm height, and 40 cm width. An iron frame surrounding all the corners of the glass tank is used to support the joints of the glass tank. The tank is divided to three chambers by Movable permeable barriers of stainless-steel meshes 0.288 mm which move in paths made at 20 cm and 120 cm from left edge of the tank.



Fig. 1 Batch experiments on coarse silica sand and mix of zeolite nano-clay with coarse silica sand 1:30 using different concentrations of iron solutions

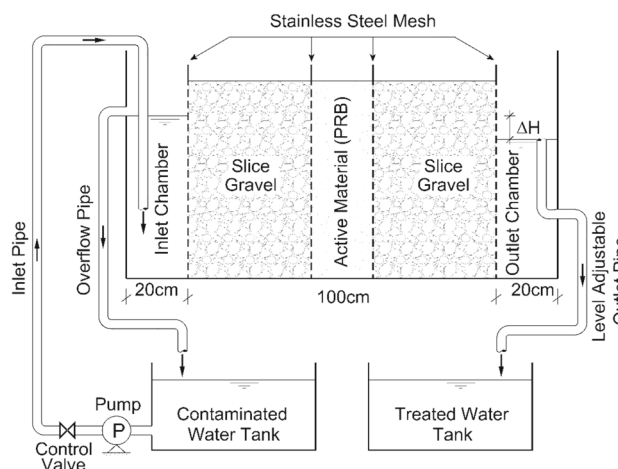


Fig. 2 A schematic for sand tank experimental model

The left chamber of the glass tank is the inlet chamber of 20 cm long. It receives the contaminated water from 500 L polyethylene tank through 1" pipe connected to a 0.5 HP centrifugal pump. A ball valve was installed after the pump to control the inlet flow. Overflow pipe of 1" diameter which acts as inlet water level control is used to drain excess water to the contaminated water tank.

The middle chamber of the glass tank is 1 m long. The middle chamber is divided to three parts by Movable permeable barriers of stainless-steel meshes 0.288 mm which move in paths made at specific distances to control the thickness of the (PRB). The active material that simulates PRB is located at the middle part which is surrounded by fine silica gravel that located in the first and third part.

The right part of the glass tank is the outlet chamber of 20 cm long. It has an outlet level adjustable pipe 1" diameter that drains the treated water to another 500 L polyethylene tank. In addition, the outlet pipe acts as overflow pipe which used to control the outlet water level and maintain a hydraulic

**Fig. 3** A 10 PRB of **a** coarse silica sand (type I), **b** mix of zeolite nano-clay and coarse silica sand (1:30) (Type II), **c** mix of zeolite nano-clay and coarse silica sand (1:15) (type III), and **d** A 25 cm PRB of mix of zeolite nano-clay and coarse silica sand (1:30) (type IV)

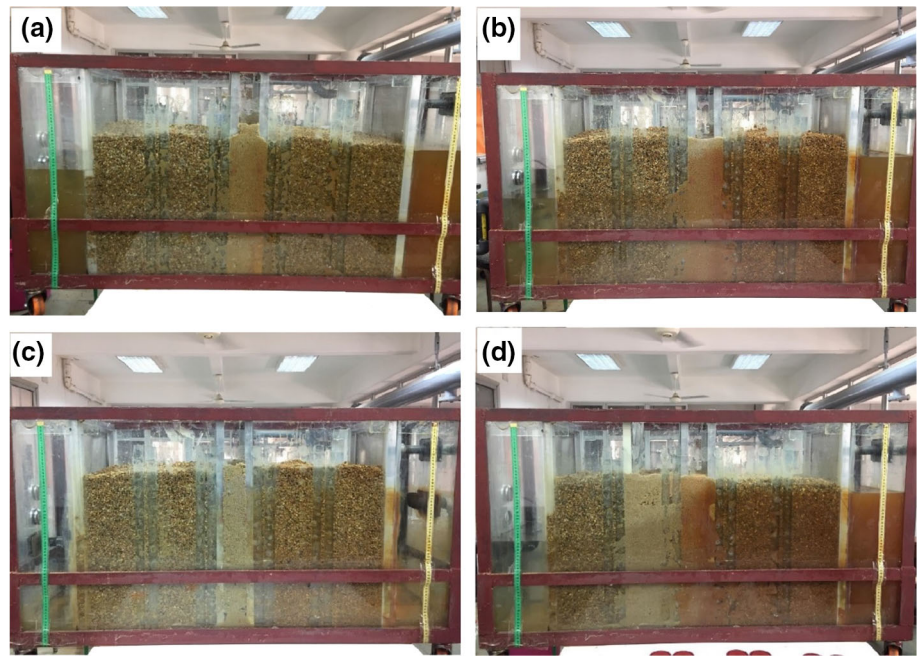


**Table 1** Iron removal efficiency ( $\eta$ ) for different media

Type of sand	$C_i$ (mg/l)	$C_f$ (mg/l)	$\eta$ (%)
Coarse silica sand (0.7–1.25 mm)	15	8.83	41.13
	20	10.87	45.65
	25	12.83	48.68
	30	16.49	45.03
	35	14.09	59.74
	40	15.25	61.88
	50	17.79	64.42
Mix of nano-clay and coarse silica sand 1:30	30	0.08	99.72
	40	0.09	99.77
	50	0.11	99.79
	60	0.19	99.68
	70	0.24	99.66

gradient due to the difference in water levels between inlet and outlet chambers. The outlet level adjustable pipe enables for changing the value of the outlet head and thus changing the value of hydraulic gradient. Figure 2 illustrates a schematic for sand tank experimental model.

The contaminated water flows through the silica gravel media and then through the active material which acts as PRB to the other side of the silica gravel media and finally to the outlet chamber of the glass tank. Four different types of active materials and thicknesses representing PRB were used to investigate the effect of different parameters as shown in Fig. 3. Thirty kgs of coarse silica sand were used to

form 10 cm thickness PRB (Type I). A ratio 1:30 of zeolite nano-clay and coarse silica sand were used to form PRBs of thicknesses 10 cm (type II) and 25 cm (type IV), respectively. For type III, two kg of zeolite nano-clay were mixed with thirty kgs of coarse silica sand (1:15) to form 10 cm thickness PRB.

The sand tank experiment is used to investigate the effects of head difference, iron concentration, contact time, nano-clay dosage, and thickness of permeable reactive barrier on the iron removal efficiency.

## 4 Results and Discussion

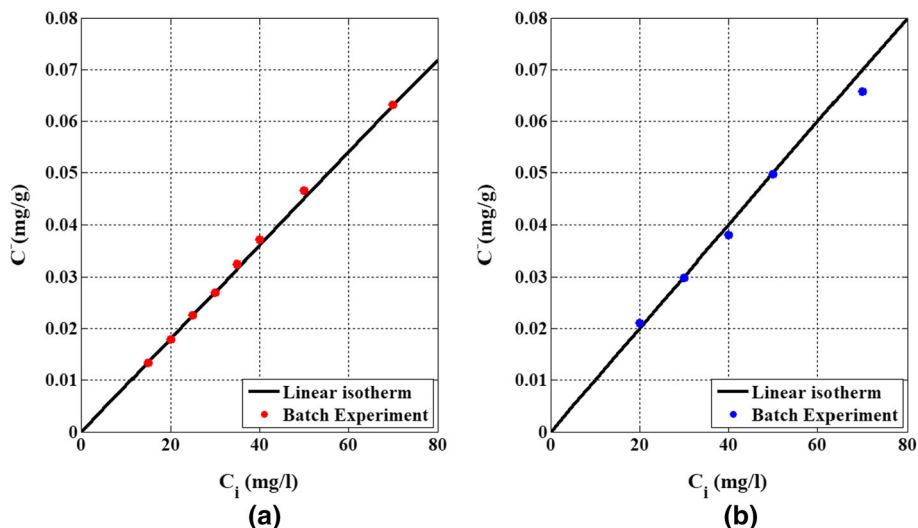
### 4.1 Batch Experiments

The following Equation is used to calculate iron removal efficiency ( $\eta$ )

$$\eta = \left( \frac{C_i - C_f}{C_i} \right) \% \quad (1)$$

where  $C_i$  and  $C_f$  are the initial and final iron concentration in the solution in (mg/l), respectively. Table 1 presents iron removal efficiency for coarse silica sand and a mix of zeolite nano-clay with ratio 1:30. It can be seen from the table that the average iron removal efficiency ( $\eta$ ) for coarse silica at concentrations ranging from 15 to 70 mg/l is around 51.87% after one hour of shaking time and 24 h of reaction. Moreover, mixing zeolite nano-clay with coarse silica sand significantly improves iron removal efficiency to almost 100% at concentrations ranging from 30 to 70 mg/l. So, it

**Fig. 4** Linear adsorption isotherm for iron onto **a** Coarse silica sand **b** Mix of nano-clay and coarse silica sand 1:30



can be used for removing iron from water to reach the safety value (below 0.3 ppm) for drinking water as instructed by EPA. On the other hand, fine silica gravel failed to reduce iron concentration in water so it could perfectly mimic non-reactive underground strata which can be used in the sand tank experiment.

Figure 4 shows the relation between adsorbed concentration (adsorbed mass of iron with respect to the mass of the media) ( $\bar{C}$ ) in (mg/g) and the initial concentration of iron solution ( $C_i$ ) in mg/l. It can be noted from the figure that by increasing solute initial concentrations, the adsorbed concentration increases with a linear relationship. Thus, the linear adsorption isotherm is the most representative for the adsorption of iron onto coarse silica sand and mix of nano-clay and coarse silica sand with distribution coefficients (slope) equal 0.0009 and 0.001, respectively.

## 4.2 Sand Tank Experiments

### 4.2.1 Effect of Sampling Time

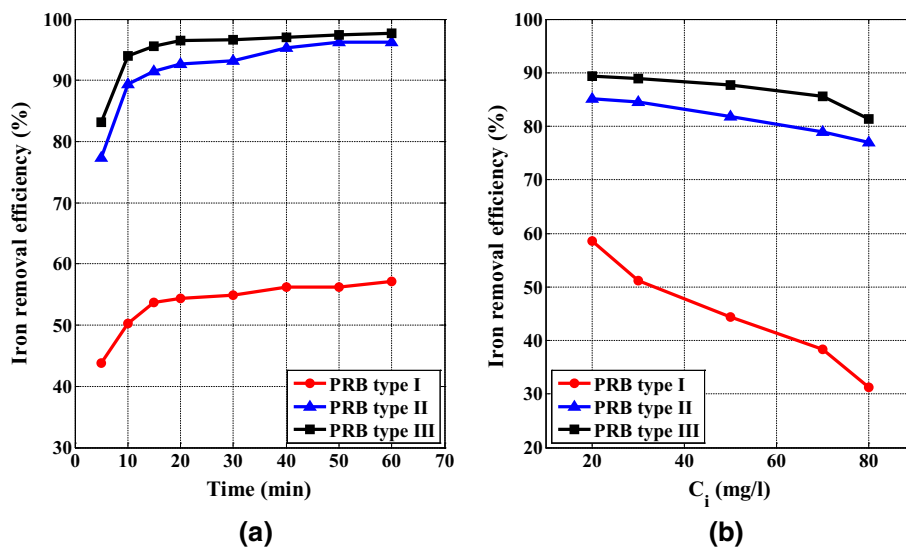
The samples were extracted from the outlet of sand tank experiment at different times ranging from 5 to 60 min measured from starting the experiment while the initial concentration of iron was 30 ppm, the head difference was 4 cm, and PRB thickness was 10 cm. The experiment was repeated three times for the three types of PRB media: coarse silica sand (type I), mix of zeolite nano-clay and coarse silica sand with ratios 1:30 (type II) and 1:15 (Type III). Figure 5a shows the iron removal efficiency ( $\eta$ ) for different media of PRB at different sampling times. It can be seen from the figure that the iron removal efficiency increases in the first 15 min then remains almost constant till the end of the experiments for the three types of PRB media. It can be attributed to unsteady state condition that exist during this period where

the sand tank is being filled and head difference is relatively large thus flow velocity increases and contact time decreases. After 15 min from starting the experiment, the flow turns to steady condition and the flow velocity and contact time are constant. One can conclude that, samples should not be taken before 15 min from stating the experiment to insure the steady state condition. It can be noticed also from the figure that the iron removal efficiency after 60 min reach 96% and 98% for PRB of mix of zeolite nano-clay and coarse silica sand with ratios 1:30 and 1:15, respectively.

### 4.2.2 Effect of Initial Concentration of Iron

The effect of changing initial iron concentration on iron removal efficiency is investigated for three different media of permeable reactive barrier (PRB). Different values of initial iron concentration ( $C_i$ ) was used from 20 to 80 mg/l while the head difference between the inlet flow and the outlet flow was maintained at 15 cm. Samples were extracted from the outlet after 30 min of starting the experiment which was conducted three times for each value of initial iron concentration for three different media of PRB with 10 cm thickness; coarse silica sand (type I), mix of nano-clay and coarse silica sand with ratios 1:30 (type II) and 1:15 (type III). Figure 5b presents the iron removal efficiency for different media of PRB and different initial concentration of iron ( $C_i$ ). It could be noticed from figure that for coarse silica sand PRB (type I), by increasing iron initial concentration from 20 to 80 mg/l the removal efficiency of iron decreases from 58 to 31%. It can be seen also that by using a mix of zeolite nano-clay and coarse silica sand with a ratio 1:30 as the media of the PRB (type II), significant improvement in the removal efficiency is achieved which increased from 58 to 85% at  $C_i = 20$  ppm and from 31 to 76% at  $C_i = 80$  ppm if it is compared to the coarse silica sand PRB. In addition, the drop in the removal

**Fig. 5** Iron removal efficiency for different media of PRB **a** at different sampling times, and **b** different initial concentration of iron ( $C_i$ )



efficiency resulted from increasing initial concentration from 20 to 80 mg/l decreases from about 30% for the silica sand PRB to nearly 10% for a mix of zeolite nano-clay and coarse silica sand (1:30) PRB. Finally, for the conducted experiments using a mix of zeolite nano-clay and coarse silica sand with a ratio 1:15 (type III), the results show that increasing nano-clay dosage increases the removal efficiency about 6% for almost all values of initial iron concentration examined if it is compared by a mix of zeolite nano-clay and coarse silica sand with a ratio 1:30 (type II). Adding zeolite nano-clay to the silica sand increases the surface area of the mix due to its small particle size, so it could adsorb larger amounts of iron at high concentrations that increases iron the removal efficiency.

Table 2 shows the initial and final iron concentrations, and iron removal efficiency for different media of PRB. It can be seen from the table that for the three media of BRB the final iron concentration increases by increasing the initial iron concentration but the iron removal efficiency decreases.

#### 4.2.3 Effect of Head Difference

Sand tank experiment was conducted several times for different values of head difference between the inlet and the outlet ranging from 4 to 15 cm and for three types of PRB media: coarse silica sand (type I), mix of zeolite nano-clay and coarse silica sand with ratios 1:30 (type II) and 1:15 (type III). The initial concentration of iron was 30 ppm, samples were extracted from the outlet after 30 min of starting the experiment, and 10 cm PRB thickness. Figure 6a shows the iron removal efficiency ( $\eta$ ) for different media of PRB and different Head difference. It can be noticed from the figure that for coarse silica sand PRB (type I), increasing head difference from 4 to 15 cm slightly decreases iron removal

efficiency from 54 to 51% as a result of increased flow velocity and thus decreases contact time between iron and active media which causes a decrease in the iron removal efficiency. Mixing zeolite nano-clay with coarse silica sand with a ratio 1:30 (type II) significantly increases the removal efficiency to 92% at 4 cm head difference and to 84% at 15 cm head difference as a result of increased surface area that causes a significant increase in sorption capacity. Finally, doubling the amount of zeolite nano-clay dosage (type III) increases the removal efficiency to reach 96% and 89% at 4 and 15 cm head differences, respectively.

#### 4.2.4 Effect of PRB Thickness

The effect of changing PRB thickness on iron removal efficiency is investigated for different values of initial iron concentration. PRB of a mix of nano-clay and coarse silica sand with a ratio 1:30 and thickness of 10 (type II) and 25 cm (type IV) are used. Figure 6b presents the iron removal efficiency ( $\eta$ ) for 10 and 25 cm thickness PRB for different iron initial concentration ( $C_i$ ). It can be seen from the figure that increasing the thickness of PRB increases iron removal efficiency about 15%. It can be attributed to increasing the surface area and the contact time between contaminant and PRB media which increases the sorption of contaminant on the surface area of the PRB media.

#### 4.2.5 Effect of Hydraulic Gradient

The effect of changing the hydraulic gradient on iron removal efficiency is investigated for 10 and 25 cm thickness PRB of a mix of nano-clay and coarse silica sand with a ratio 1:30. Table 3 presents iron removal efficiency for two values of hydraulic gradient (0.4 and 0.6). It can be noted from the table

**Table 2** The initial and final iron concentrations and iron removal efficiency for different media of PRB

$C_i$ (mg/l)	Coarse silica sand			Mix nano-silica (1:30)			Mix nano-silica (1:15)		
	$C_f$ (mg/l)	$C_i - C_f$ (mg/l)	% Removal	$C_f$ (mg/l)	$C_i - C_f$ (mg/l)	% Removal	$C_f$ (mg/l)	$C_i - C_f$ (mg/l)	% Removal
20	8.30	11.70	58.50	2.96	17.04	85.20	2.12	17.88	89.42
30	14.63	15.37	51.24	4.65	25.35	84.51	3.34	26.66	88.85
50	27.84	22.16	44.33	9.08	40.93	81.85	6.12	43.88	87.76
70	43.17	26.83	38.34	14.70	55.30	79	10.14	59.86	85.52
80	55.00	25.00	31.25	18.46	61.54	76.93	14.90	65.10	81.38

**Fig. 6** Iron removal efficiency **a** for different media of PRB and different head difference and, **b** for 10 and 25 cm PRB thickness and different initial concentration of iron ( $C_i$ )

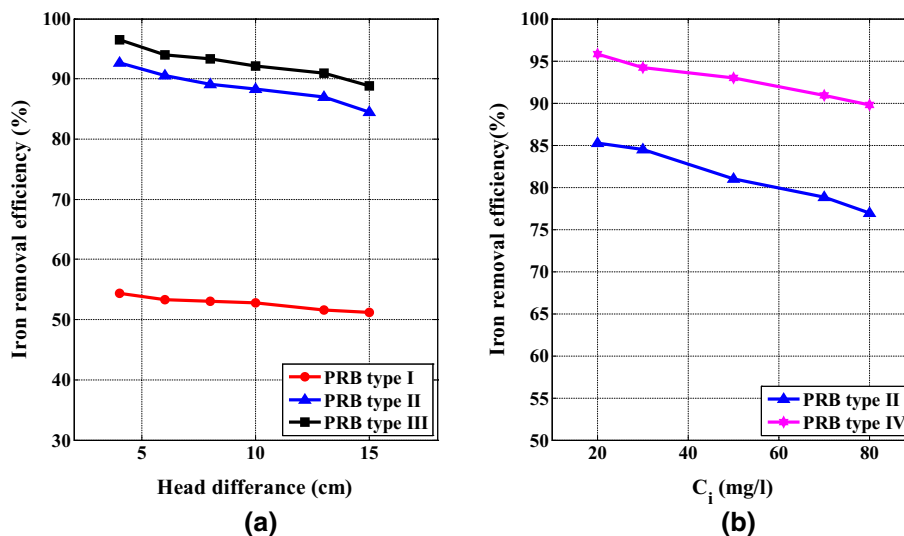


**Table 3** Effect of changing PRB thickness on the removal efficiency for two hydraulic gradients

Gradient = 0.4	% Removal	Gradient = 0.6	% Removal
$\Delta H = 4$ cm Thickness 10 cm	92.61	$\Delta H = 6$ cm Thickness 10 cm	92.33
$\Delta H = 10$ cm Thickness 25 cm	95.88	$\Delta H = 15$ cm Thickness 25 cm	94.19

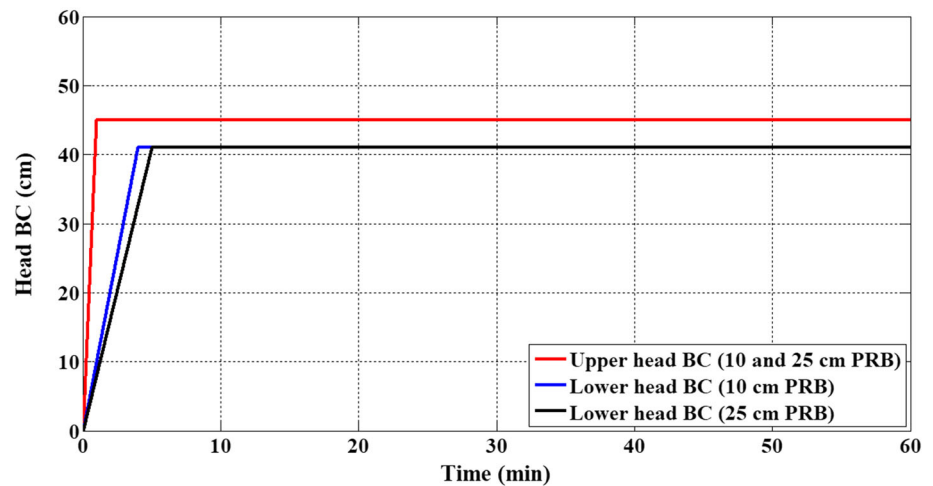
that for the same thickness of PRP, increasing the hydraulic gradient by 50% decrease iron removal efficiency but with insignificant value. It can be attributed to increasing the contact time between contaminant and PRB media. It can be noticed also from the table that for the same value of hydraulic gradient, increasing the thickness of the PRB increases iron removal efficiency which attributed to increased surface area of PRB media and the contact time between contaminant and PRB media.

### 4.3 Numerical Contaminant Transport Model Verification

In this section, the experimental model data were used to evaluate the capability of a numerical contaminant transport model to reproduce the experimental results. The MT3DMS numerical model [21] included within the Groundwater Modeling System (GMS) was used along with the different experimental data to obtain reaction rate values for linear isotherms.

MT3DMS is a three-dimensional multi-species solute transport model for simulating contaminant transport in saturated groundwater flow systems [21, 22]. MT3DMS interfaces directly with the US Geological Survey finite-difference groundwater flow model MODFLOW for the flow solution and supports the hydrologic and discretization features of MODFLOW [23]. MT3DMS has been widely used in research projects and practical field applications. Both MT3DMS and MODFLOW are packages within the Groundwater Modeling System (GMS) that is a user-friendly interface to deal with such models.

**Fig. 7** Head boundary conditions for a 10 and 25 cm PRB



#### 4.3.1 Groundwater Flow Model

Three groundwater flow models were built using 3D grid in GMS. The first model simulating coarse silica sand PRB with thickness 10 cm. the second and third models for PRB of a mix of zeolite nano-clay and coarse silica sand with ratios 1:30 and 1:15, respectively. The used grid size is 1 cm  $\times$  1 cm with variable head boundary at upper and lower edges of the models and no flow boundary at east and west edges. Figure 7 shows the variable head boundary conditions of the models that simulate the transient conditions during the filling of the sand tank experiment. It can be seen from the figure that, for upper and lower boundaries of 10 cm PRB, the head increases from zero to 0.45 m in one minute and from zero to 0.41 m in four minutes and then remain constant to the end of simulation. The third model has the same upper boundary condition while the lower boundary condition change to simulate the increased filling time to reach 5 min due to the increase in PRB thickness to 25 cm. The bottom layer of the model is represented as impervious layer to simulate the base of sand tank. Simulation time was 60 min. The porosities for gravel and coarse silica sand are 0.55 and 0.35 which were obtained experimentally. Also, the hydraulic conductivities were obtained experimentally using constant head test. The values of hydraulic conductivity for gravel, coarse silica sand and a mix of zeolite nano-clay and coarse silica sand are 0.07 m/s, 0.00605 m/s, and 0.001 m/s, respectively.

Figure 8 shows a color filled head contours in plan view for the model at steady state for a 10 cm coarse silica sand PRB. The cells in the middle ten rows represent the 10 cm-thickness PRB of coarse silica sand while the rest of the cells represents the gravel media in sand tank experiment. It can be seen from the figure that the reduction in the head is very low upstream and downstream the PRB because of the

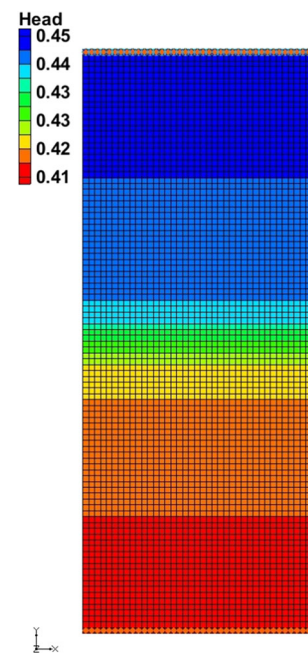


**Fig. 8** Color fill head contours in plan for 10 cm coarse silica sand PRB

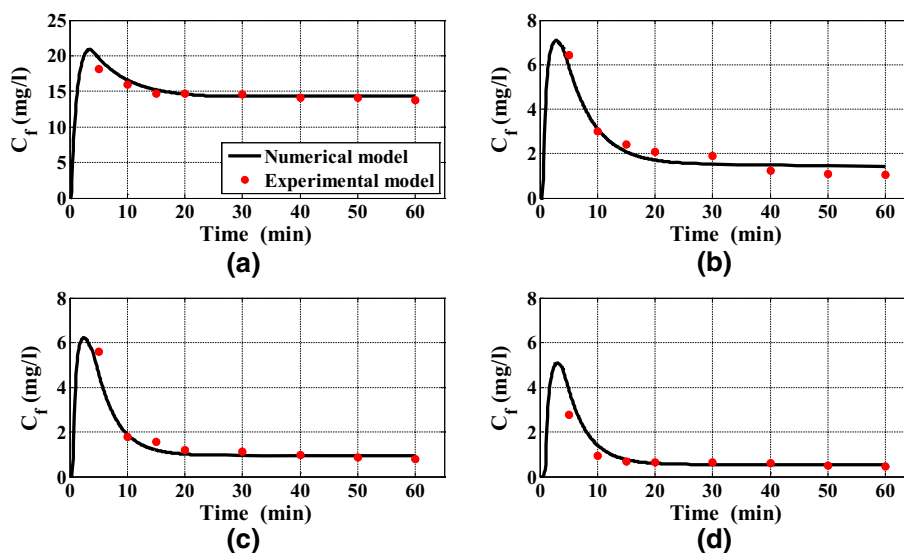
high value of hydraulic conductivity in these regions which simulates the gravel media in the sand tank experiment.

#### 4.3.2 Contaminant Transport Model

After building the transient flow models and obtaining the head values, the contaminant transport simulations were conducted using MT3DMS [21]. The models simulating the transport process through coarse silica sand PRB with thickness 10 cm and a mix of zeolite nano-clay and coarse silica sand with thicknesses 10 and 25 cm. The main objective of these simulations is to investigate the capability of Linear isotherm to predict the results obtained from the experimental model and obtaining adsorption isotherms constants. The



**Fig. 9** Concentration breakthrough curves of the experimental model and the numerical model for different media of PRB



kinetic formulation for the Linear isotherm is as follows

$$\frac{\partial C}{\partial t} = K_r(K_d C - \bar{C}) = K_f C - K_b \bar{C} \tag{2}$$

where  $K_r$  is the reaction rate constant ( $T^{-1}$ ),  $K_f$  is the forward reaction coefficient,  $K_b$  is the backward reaction coefficient. If  $K_r$  reaches  $\infty$  the kinetic formulation returns to the equilibrium formulation.

The chemical reaction package was used to simulate the adsorption of iron onto the media of the PRB. The longitudinal dispersivity of the PRB and gravel layers were taken 3 m and 6 m, respectively [24, 25]. The advection package used was third order total variation diminishing (TVD) scheme. The northern boundary of the model was set as a permanent source of contamination with 30 mg/l and the outlet concentration is obtained at the southern boundary of the model through the 60-min simulation time. The linear adsorption isotherm was constructed simultaneously with first order kinetic reactions. The values of the adsorption isotherm and kinetic rate reaction constant were adjusted manually to obtain the best representation of the experimental adsorption isotherm.

Concentration breakthrough curves of the experimental model and the numerical model for Linear Isotherm are presented in Fig. 9. It can be seen from the figure that the final concentrations of iron increase in the first 4 min due to the transient state during the filling of the tank then gradually decline after 20 min then remain almost constant till the end of simulation time. The values of adsorption isotherms constants used to fit the experimental data alongside with kinetic reaction constants are indicated in Table 4.

Figures 10 shows a color filled concentration contours in plan view for the model at the end of simulation time. The cells in the middle rows represent the PRB while the rest of

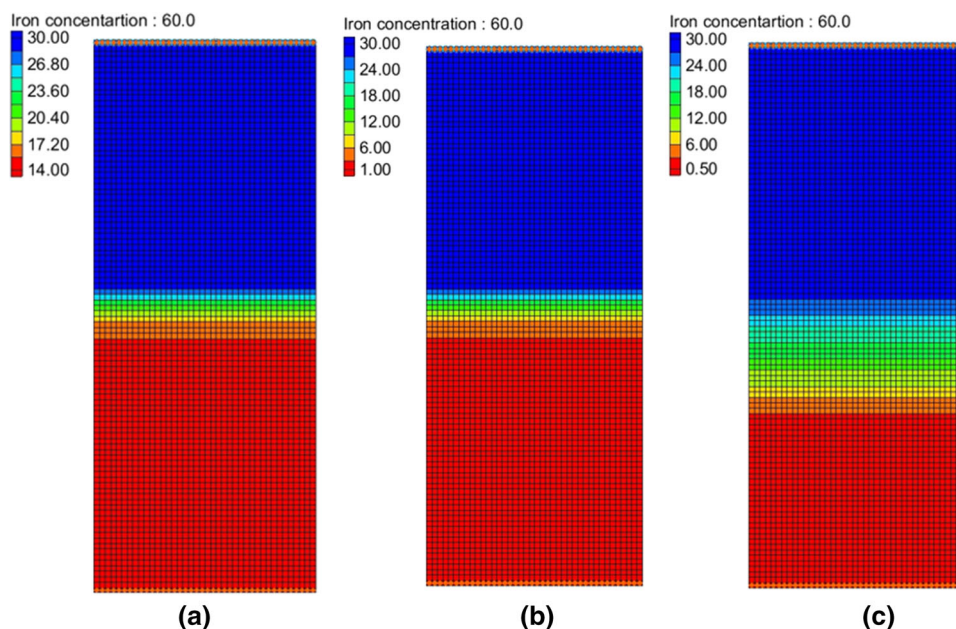
**Table 4** Adsorption isotherm and reaction rate constants used to best fit the experimental data for different media of PRB

Media of PRB	1st sorption const	Reaction rate const
10 cm coarse silica sand	0.08	0.085
10 cm mix nano-clay and silica sand 1:30	0.1	0.2
10 cm mix nano-clay and silica sand 1:15	0.1	0.28
25 cm mix nano-clay and silica sand 1:30 PRB	0.03	0.18

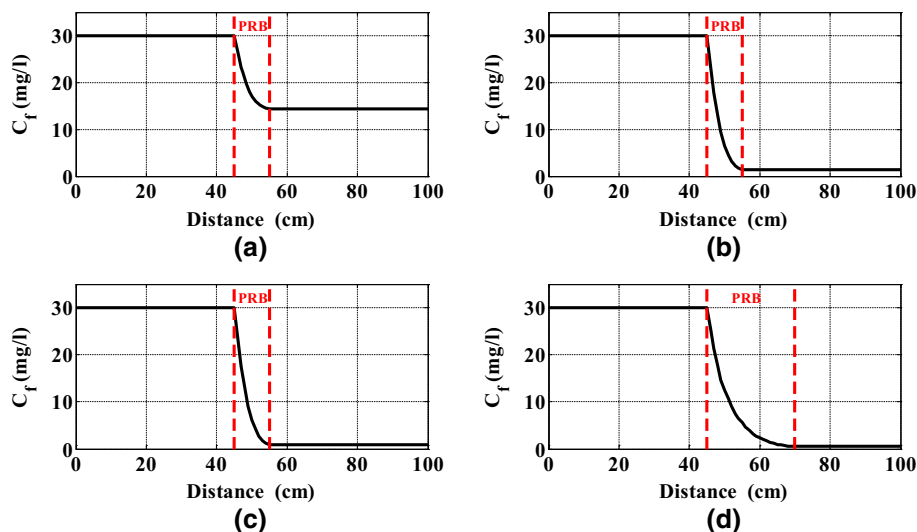
the cells represent the gravel media in sand tank experiment. It can be seen from the figure that the adsorption of iron occurs mainly in the cells representing the PRB layer as Iron concentrations reduces from 30 ppm to about 14, 1 and 0.5 ppm for a 10 cm PRB of coarse silica sand, 10 cm, and 25 cm PRB of mix of nano-clay and silica sand 1:30, respectively while the gravel layers did not reduce iron concentrations. The mix layer significantly improved the adsorption of iron onto the PRB. Moreover, increasing thickness of PRB decreased concentration gradient, so the reduction in iron concentration occurred over larger distance.

Figure 11 presents the concentration profile at the end of simulation time for different media of PRB. It can be seen from the figure that iron concentration remains constant at 30 mg/l through the upstream gravel layer which starts from station 0 to station 45 cm. Then, iron concentration significantly decreases through PRB layer. Then, it remains almost constant through the downstream gravel layer simulating the experimental model. By comparing Fig. 11a with Figs. 11b–d one can note that, the drop in iron concentration through the

**Fig. 10** Color fill concentration contours in plan for **a** 10 cm PRB of coarse silica sand, **b** 10 cm PRB of mix of nano-clay and silica sand PRB, **c** 25 cm PRB of mix of nano-clay and silica sand 1:30



**Fig. 11** The concentration profile at the end of simulation for PRB **a** type I, **b** type II, **c** type III, and **d** type IV



PRB of a mix of nano-clay and coarse silica sand is significantly larger than for coarse silica sand PRB. The drop also slightly increases as the mix ratio of nano-clay and coarse silica sand increases from 1:30 to 1:15. One can also note that increasing the thickness of the PRB increases the drop in iron concentration through it and decreasing iron concentration gradient.

## 5 Summary and Conclusions

In this research, the efficiency of using zeolite nano-clay and silica sand in removing iron from groundwater is investigated experimentally as an application of in situ remediation technique using permeable reactive barrier (PRB). The study

objective was achieved through several steps. In the first step batch experiments were conducted on coarse silica sand (0.7–1.25 mm) and fine silica gravel (3–6 mm) using iron solutions with concentrations ranging from 15 to 70 mg/l to determine their iron removal efficiency from contaminated groundwater and identify the right size of silica to mix with nano-clay. The results show that the removal efficiency was about 51.87% for coarse silica sand while fine silica gravel failed to reduce the iron concentration in water. Also, batch experiments on a mix of zeolite nano-clay and coarse silica sand (1:30) were conducted using iron solutions of concentrations ranging from 30 to 70 mg/l to determine their iron removal efficiency. It is found that iron removal efficiency significantly increases to about 99.70%. The linear adsorption isotherm was found the most representative



for the adsorption of iron onto coarse silica sand and mix of nano-clay and coarse silica sand with distribution coefficients equal 0.0009 and 0.001, respectively.

The second step was to build an experimental model based on the results from the batch experiments, simulating permeable reactive barrier PRB's effect on contaminated groundwater with iron as an application of in situ remediation techniques. A glass sand tank with coarse silica sand and a mix of zeolite nano-clay and coarse silica PRBs was constructed. Sensitivity analysis on the different parameters affecting the removal efficiency (e.g., initial concentration of iron, head difference, sampling time, nano-clay dosage, and thickness of PRB) was conducted. The initial concentration of iron was changed from 20 to 80 ppm. Head difference was changed from 4 to 15 cm to investigate the effect of contact time. Samples were extracted from the effluent tank at different times within an hour. Nano-clay dosage was increased from one to 2 kg to achieve ratios of 1:30 and 1:15 of nano-clay to coarse silica sand in the mix. Finally, thickness of PRB was increased from 10 to 25 cm. The results indicated that increasing iron concentration and head difference decreases iron removal efficiency. The mix of zeolite nano-clay and coarse silica sand improves iron removal efficiency. Furthermore, increasing nano-clay dosage slightly increases the removal efficiency. However, increasing the thickness of filter layer significantly improves the removal efficiency.

In the third and final step, the experimental model data were used to test the capability of a numerical contaminant transport model to reproduce the experimental results. The MT3DMS numerical model included within the Groundwater Modeling System (GMS) was used along with the different experimental data to obtain reaction rate values for linear isotherm. The values of Linear isotherm constant that represent the best fit to the experimental data are 0.08, 0.1, 0.1 and 0.03 for a 10 cm thickness PRB of a) coarse silica sand, b) mix of zeolite nano-clay and coarse silica sand with ratio 1:30, c) mix of zeolite nano-clay and coarse silica sand with ratio 1:15 and d) a 25 cm thickness mix of zeolite nano-clay and coarse silica sand PRB, respectively.

**Open Access** This article is licensed under a Creative Commons Attribution 4.0 International License, which permits use, sharing, adaptation, distribution and reproduction in any medium or format, as long as you give appropriate credit to the original author(s) and the source, provide a link to the Creative Commons licence, and indicate if changes were made. The images or other third party material in this article are included in the article's Creative Commons licence, unless indicated otherwise in a credit line to the material. If material is not included in the article's Creative Commons licence and your intended use is not permitted by statutory regulation or exceeds the permitted use, you will need to obtain permission directly from the copyright holder. To view a copy of this licence, visit <http://creativecommons.org/licenses/by/4.0/>.

## References

- Dawodu, F.A.; Akpomie, K.G.: Simultaneous adsorption of Ni(II) and Mn(II) ions from aqueous solution unto a Nigerian kaolinite clay. *J. Market. Res.* **3**(2), 129–141 (2014). <https://doi.org/10.1016/j.jmrt.2014.03.002>
- Simon, F.; Biermann, V.: Groundwater remediation using permeable reactive barriers. *Land Contam. Reclam.* **15**, 31–40 (2007). <https://doi.org/10.2462/09670513.787>
- He, Q., Si, S., Yang, J., Tu, X.: Application of permeable reactive barrier in groundwater remediation. *E3S Web Conf.* **136**, 06021 (2019). <https://doi.org/10.1051/e3sconf/201913606021>
- Ezrina, O., Suffian, Y. M., Aziz, H. A., Adlan, M. N.: The effectiveness of silica sand in semi-aerobic stabilized landfill leachate treatment. *Civil and environmental engineering faculty publications.* **386** (2010). [https://engagedscholarship.csuohio.edu/encee\\_facpub/386](https://engagedscholarship.csuohio.edu/encee_facpub/386)
- Theron, J.; Walker, J.A.; Cloete, T.E.: Nanotechnology and water treatment: applications and emerging opportunities. *Crit. Rev. Microbiol.* **34**(1), 43–69 (2008). <https://doi.org/10.1080/10408410701710442>
- Matlochová, A.; Plachá, D.; Rapantová, N.: The application of nanoscale materials in groundwater remediation. *Pol. J. Environ. Stud.* **22**(5), 1401–1410 (2013)
- Amin, M.T.; Alazba, A.A.; Manzoor, U.: A review of removal of pollutants from water/wastewater using different types of nanomaterials. *Adv. Mater. Sci. Eng.* (2014). <https://doi.org/10.1155/2014/825910>
- Tratnyek, P.G.; Johnson, R.L.: Nanotechnologies for environmental cleanup. *Nano Today* **1**(2), 44–48 (2006). [https://doi.org/10.1016/S1748-0132\(06\)70048-2](https://doi.org/10.1016/S1748-0132(06)70048-2)
- Nowack, B.; Bucheli, T.D.: Occurrence, behavior and effects of nanoparticles in the environment. *Environ. Pollut.* **150**(1), 5–22 (2007). <https://doi.org/10.1016/j.envpol.2007.06.006>
- Zhang, W.: Nanoscale iron particles for environmental remediation: an overview. *J. Nanopart. Res.* **5**(3–4), 323–332 (2003)
- Lien, H.; Zhang, W.: Nanoscale iron particles for complete reduction of chlorinated ethenes. *Colloids Surf. A* **191**(1–2), 97–105 (2001). [https://doi.org/10.1016/S0927-7757\(01\)00767-1](https://doi.org/10.1016/S0927-7757(01)00767-1)
- Lien, H.; Zhang, W.: Hydrodechlorination of chlorinated ethanes by nanoscale Pd/Fe bimetallic particles. *J. Environ. Eng.* **131**(1), 4–10 (2005). [https://doi.org/10.1061/\(ASCE\)0733-9372\(2005\)131:1\(4\)](https://doi.org/10.1061/(ASCE)0733-9372(2005)131:1(4))
- Prabhakar, V.; Bibi, T.: Nanotechnology, future tools for water remediation. *Int. J. Emerg. Technol. Adv. Eng.* **3**(7), 54–59 (2013)
- Klimkova, S.; Cernik, M.; Lacinova, L.; Filip, J.; Jancik, D.; Zboril, R.: Zero-valent iron nanoparticles in treatment of acid mine water from in situ uranium leaching. *Chemosphere* **82**(8), 1178–1184 (2011). <https://doi.org/10.1016/j.chemosphere.2010.11.075>
- Hamza, H.A., Atieh, M.A., Laoui, T.: Removal of phenol by carbon nanotubes and activated carbon-comparative analysis. In: Sixteenth international water technology conference, Istanbul, Turkey, 1–7 (2012)
- Elsehly, E.M.I.; Chechenin, N.G.; Bukunov, K.A.; Makunin, A.V.; Priselkova, A.B.; Vorobyeva, E.A.; Motaweh, H.A.: Removal of iron and manganese from aqueous solutions using carbon nanotube filters. *Water Sci. Technol. Water Supply* **16**(2), 347–353 (2016)
- Naghizadeh, A.; Nasser, S.; Nazmara, S.: Removal of trichloroethylene from water by adsorption on to multiwall carbon nanotubes. *Iranian J. Environ. Health Sci. Eng.* **8**(4), 317–324 (2011)
- Qu, G.; Kou, L.; Wang, T.; Liang, D.; Hu, S.: Evaluation of activated carbon fiber supported nanoscale zero-valent iron for chromium (VI) removal from groundwater in a permeable reactive column. *J. Environ. Manage.* **201**, 378–387 (2017)



19. Parisi, F.; Lazzara, G.; Merli, M.; Milioto, S.; Princivalle, F.; Sciascia, L.: Simultaneous removal and recovery of metal ions and dyes from wastewater through montmorillonite clay mineral. *Nanomaterials* **9**(12), 1699 (2019). <https://doi.org/10.3390/nano9121699>
20. Chen, X.; Yu, L.; Zou, S.; Xiao, L.; Fan, J.: Zeolite cotton in tube: a simple robust household water treatment filter for heavy metal removal. *Sci Rep* **10**(1), 4719 (2020). <https://doi.org/10.1038/s41598-020-61776-8>
21. Zheng, C., Wang, P.P.: MT3DMS-a modular three-dimensional multispecies transport model strateg. *Environ. Res. Dev. Progr.* 1–40 (1999).
22. Zheng, C.; Hill, M.C.; Cao, G.; Ma, R.: MT3DMS: Model use, calibration, and validation. *Trans. ASABE* **55**(4), 1549–1559 (2012). <https://doi.org/10.13031/2013.42263>
23. Zheng, C., Hill M.C., Hsieh P.A.: MODFLOW-2000, the U.S. Geological Survey modular ground-water model - user's guide to the LMT6 package, the linkage with MT3DMS for multi-species mass transport modeling, U.S. Geological Survey Open-File Report 01–82, 43 (2001)
24. Adams, E.E.; Gelhar, L.W.: Field study of dispersion in a heterogeneous aquifer: 4. Investigation of adsorption and sampling bias. *Water Resour. Res.* **28**(12), 3325–3336 (1992)
25. Lønborg, M.J.; Engesgaard, P.; Bjerg, P.L.; Rosbjerg, D.: A steady state redox zone approach for modeling the transport and degradation of xenobiotic organic compounds from a landfill site. *J. Contam. Hydrol.* **87**(3–4), 191–210 (2006)

